Regular Article

Delayed feedback control of phase synchronisation in a neuronal network model

Michele Mugnaine[1], Adriane S. Reis[2], Fernando S. Borges[3], Rafael R. Borges[4], Fabiano A. S. Ferrari[5], Kelly C. Iarosz[6,7,8], Ibere L. Caldas[6], Ewandson L. Lameu[7,9], Ricardo L. Viana[2,a], Jose D. Szezech, Jr.[1,10], Jürgen Kurths[7,8], and Antonio M. Batista[1,8,10]

[1] Graduate in Science Program, State University of Ponta Grossa, Ponta Grossa, PR, Brazil
[2] Physics Department, Federal University of Paraná, Curitiba, PR, Brazil
[3] Center for Mathematics, Computation, and Cognition, Federal University of ABC, São Bernardo do Campo, SP, Brazil
[4] Department of Mathematics, Federal Technological University of Paraná, Ponta Grossa, PR, Brazil
[5] Federal University of Vales of Jequitinhonha and Macuri, Institute of Engineering, Science and Technology, Janaúba, MG, Brazil
[6] Physics Institute, University of São Paulo, São Paulo, SP, Brazil
[7] Department of Physics, Humboldt University, Berlin, Germany
[8] Potsdam Institute for Climate Impact Research, Potsdam, Germany
[9] National Institute for Space Research, São José dos Campos, SP, Brazil
[10] Department of Mathematics and Statistics, State University of Ponta Grossa, PR, Brazil

Abstract. The human cerebral cortex can be separated into cortical areas forming a clustered network structure. We build two different clustered networks, where one network is based on a healthy brain and the other according to a brain affected by a neurodegenerative process. Each cortical area has a subnetwork with small-world properties. We verify that both networks exhibit rich-club organisation and phase synchronisation. Due to the fact that neuronal synchronisation can be related to brain diseases, we consider the delayed feedback control as a method to suppress synchronous behaviours. In this work, it is presented that depending on the feedback parameters, intensity and time delay, phase synchronisation in both networks can be suppressed. Therefore, one of our main results is to show that delayed feedback control can be used to suppress undesired synchronous behaviours not only in the healthy brain, but also in the brain marked by neurodegenerative processes.

[a] e-mail: viana@fisica.ufpr.br

1 Introduction

The brain is an organ composed of neurons which are interconnected through electrical and chemical synapses [1,2]. Both kinds of synapses transmit information, but by different mechanisms. Electrical synapse is a conductive link between neighbouring neurons, where the signal transmission can happen in both directions and it is extremely fast [3]. In the chemical synapse, the signal transmission is directed and slower than the electrical synapse [4].

In mammals, the brain varies in size, and it has functional and anatomical distinct structures [5]. The largest part of the human brain is the cortex, responsible for important functions, such as thought, cognition, and memory [6]. The cortex regions are densely interconnected by means of cortical axonal pathways [7]. Thomas et al. [8] estimated the organisation of the human cerebral cortex by intrinsic functional connectivity. They reported that different regions exhibit distinct features. Glasser et al. [9] used multi-modal magnetic resonance images from the Human Connectome Project to delineate and characterise cortical areas.

Phase synchronisation plays an important role in memory processes [10]. However, neuronal synchronisation can be associated with brain disorders, for example epilepsy [11,12] and Parkinson's disease [13,14]. Lameu et al. [15,16] analysed not only synchronous behaviour, but also suppression of bursting synchronisation in clustered neuronal networks and in networks based on cat's brain. They analysed different interventions to suppress phase synchronisation, such as external time-periodic driving and delayed feedback control.

Delayed feedback control was introduced by Pyragas [17] as a method of chaos control. This method has many applications in various dynamical systems, such as Duffing–van der Pol oscillator [18], quasi-integrable Hamiltonian systems [19], and economical model [20]. Rosenblum and Pikovsky [21] suggested a method based on delayed feedback that can be applied to suppress pathological rhythms in neuronal systems. Batista et al. [22] investigated the suppression of bursting synchronisation in scale-free networks of Rulkov neurons using delayed feedback control. Feedback signal was also considered to suppress synchronisation in network of networks [23].

Delayed feedback was adapted for deep brain stimulation to control undesired synchronous behaviours. The deep brain stimulation is a neurological surgery involving electrical stimulation to neuronal target structures through implanted electrodes [24]. Popovych and Tass [25] studied delayed feedback for electrical brain stimulation. They used multisite linear delayed feedback to modulate the pulse amplitude of high-frequency and as a consequence to desynchronise collective rhythmic activity in a neuronal ensemble. Abnormal neuronal synchronisation can be desynchronised by means of a pulsatile electrical brain stimulation subjected to an amplitude modulation by delayed feedback strategies [26].

There are studies about the mitigation of synchronisation during epileptic activity by deep brain stimulation [27]. Recently, it was demonstrated that electrical stimulation can be used to reduce spike-and-wave episodes in epilepsy [28]. Maksimenko et al. [29] developed an algorithm for the prediction of spike-wave-discharges that are related to epileptic seizures. The absence seizure prediction algorithm indicates synchronisation within and between brain structures. This way, the delayed feedback control can be applied at the onset of a seizure.

We build neuronal networks according to the topological organisation of the structural cortical networks obtained by Lo et al. [30]. Using diffusion tensor image tractography, they constructed structural connection matrices from human brains. One obtained from a healthy patient and other from a patient with Alzheimer's disease. In our networks, we consider in each cortical area a subnetwork with small-world properties. Small-world networks have a low average characteristic path length and a high average clustering coefficient [31]. He et al. [32] provided evidence of small-world

properties in the human brain by cortical thickness from magnetic resonance imaging. With regarding to the neuron model, we utilise the Rulkov map [33], that mimics neuronal bursts and have been used to investigate coupled networks [34,35]. We apply a feedback control to this kind of coupled network and analyse alterations in the obtained synchronisation pattern due to the applied feedback control.

In this work, our contribution is to perform a comparison between two clustered networks: (i) a network built from a healthy brain, and (ii) another from a brain with a neurodegenerative disease. The networks exhibit phase synchronisation in different areas. One novel aspect is the occurrence of different synchronous patterns between the networks due to the rich-club organisation, where the rich-club is given by different areas. One of our main results is to show that the delayed feedback control leads to a successful suppression of the synchronous behaviours in both networks.

This paper is organised as follows: in Section 2, we introduce our neuronal network composed of coupled Rulkov maps. Section 3 shows that depending on the parameters the network can exhibit phase synchronisation. In Section 4, we study the effect of delayed feedback control on the synchronisation. Our final remarks are presented in the last section.

2 Neuronal network

In our network each neuron is modelled by the Rulkov map [33]

$$x_{n+1} = \frac{\alpha}{1 + x_n^2} + y_n, \tag{1}$$

$$y_{n+1} = y_n - \sigma(x_n - \beta), \tag{2}$$

where n corresponds to the interaction, x_n and y_n are the dynamical variables, α controls the spiking time-scale, and σ and β are associated with the slow time-scale. We consider $\sigma = 0.01$, $\beta = -1.25$, and α is randomly distributed in the interval $[4.1, 4.4]$. Figure 1 displays the time evolution of x_n and y_n that represent the fast and slow dynamical variables, respectively. In Figure 1a we see chaotic bursts, where the point in time when the burst starts is represented by n_k, where k is an integer. The y_n variable exhibits regular saw-teeth oscillations with local maximum and minimum when the burst starts and ends, respectively, as shown in Figure 1b.

The neuronal networks is composed of Rulkov maps and the dynamics is given by

$$x_{n+1}^{(i,a)} = \frac{\alpha^{(i,a)}}{1 + \left(x_n^{(i,a)}\right)^2} + y_n^{(i,a)} + \frac{g_e}{2}\left(x_n^{(i-1,a)} + x_n^{(i+1,a)} - 2x_n^{(i,a)}\right)$$

$$- g_c \sum_{d=1}^{D}\sum_{f=1}^{F}\left[A_{(d,f),(i,a)}H\left(x_n^{(d,f)} - \theta\right)\left(x_n^{(i,a)} - V_s\right)\right] + \Lambda_n, \tag{3}$$

$$y_{n+1}^{(i,a)} = y_n^{(i,a)} - \sigma(x_n^{(i,a)} - \beta), \tag{4}$$

where (i, a) denotes the neuron i in the area a, g_e and g_c are the electrical and chemical coupling strengths, respectively. $A_{(d,f),(i,a)}$ is the adjacency matrix of the chemical connections, $H(x)$ the Heaviside step function, θ the presynaptic threshold, V_s the reversal potential, and Λ_n is the external perturbation. We consider $\theta = -1$, $V_s = 1$ for excitatory synapses, and $V_s = -2$ for inhibitory synapses. The connectivity matrix
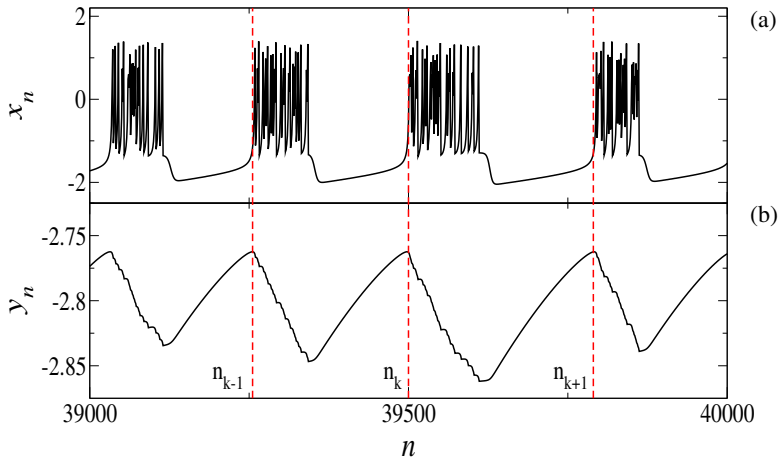
Fig. 1. Time evolution of (a) x_n and (b) y_n for the Rulkov map, where n_k denotes when the burst starts.
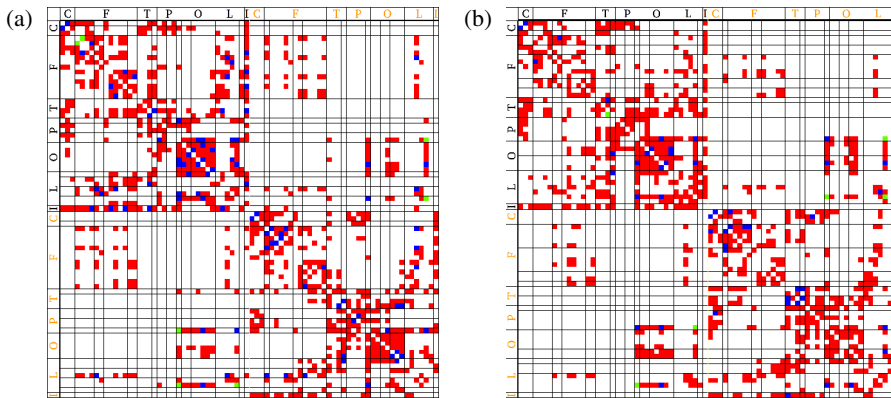

Fig. 2. Matrices of the corticocortical connectivity for (a) healthy (HM) and (b) degenerative (DM) brain, where the matrix elements have connections weighted 0 (white), 1 (red), 2 (blue), or 3 (green). The matrices have 78 areas that are separated into 7 regions (left hemisphere in black colour and right hemisphere in orange colour): central lobe (C), frontal lobe (F), temporal lobe (T), parietal lobe (P), occipital lobe (O), limbic lobe (L), and insula (I).

has $F = 78$ areas and each area has a subnetwork with $D = 100$ neurons, where the subnetwork is constructed according to the Newman–Watts network [36].

The adjacency matrix $A_{(d,f),(i,a)}$ is based on the topological organisation in the structural cortical networks obtained by Lo et al. [30]. Figures 2a and 2b show the matrices for the healthy (HM) and degenerative (DM) brain, respectively. The matrix elements have connections weighted 0 (white), 1 (red), 2 (blue), or 3 (green). We consider 0, 1, 2, and 3 for absent, sparse, intermediate, and dense connection, respectively.

We calculate the matching index (MI) for both HM and DM, due to the fact that a large MI value is associated with synchronous behaviour. The MI is obtained by means of the connectivity MI $m_{aa'}$ between two areas a and a' ($a \neq a'$). $m_{aa'}$ is the
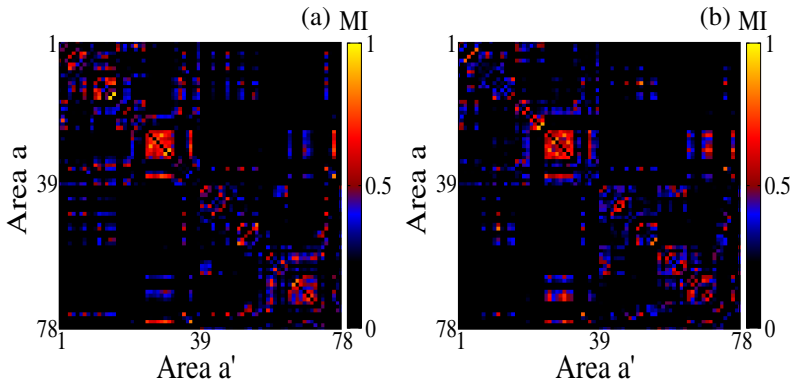
Fig. 3. Normalised matching index for all areas from the (a) HM and (b) DM.

amount of overlap of their neighbourhoods, and given by [37]

$$m_{aa'} = M_{aa'} + \sum_{n=1}^{N} M_{an} M_{a'n}, \tag{5}$$

where $M_{aa'}$ is the adjacency matrix with elements equal to 1 when a and a' are connected and 0 when they are not connected. We normalise MI dividing each element by $k_a + k_{a'} - m_{aa'}$, where k_a is the degree of the area a. $m_{aa'} = 1$ if all inputs to areas a and a' come from different areas, and $m_{aa'} = 0$ if they receive inputs from the same areas. In Figure 3, we see that both HM and DM have a group of areas ($26 \leq a \leq 32$) with high MI values, that corresponds to the occipital region in the brain.

We analyse the connectivity profile of both matrices by means of the weighted rich-club parameter, that is given by [38]

$$\rho(r) = \frac{\phi(r)}{\phi_{\text{random}}(r)}, \tag{6}$$

where

$$\phi(r) = \frac{W_{>r}}{\sum_{l=1}^{E_{<r}} w_l^{\text{rank}}}, \tag{7}$$

where r is the richness index calculated from the sum of the weights attached to the connections originating from a neuron, E the total number of connections, and w_l^{rank} is the ranked weight with $w_l^{\text{rank}} \leq w_{l+1}^{\text{rank}}$ ($l = 1, 2, 3, \ldots, E$). A network has a rich-club organisation if $\rho(r)$ is greater than 1 over a range r. We verify that both HM and DM have a rich-club organisation. Figure 4 shows ρ for the HM (black circles) and DM (red triangles) brain, and as a result we identify the areas with higher ρ values which are the most interconnected ones (local rich-club). In the HM (black circles), the rich-club is composed of the areas 25, 29, 30, 37, 64, and 76. The rich-club in the DM (red triangles) is given by the areas 25, 37, 64, 69, and 76. Therefore, both networks have rich-club organisation composed of different areas due to the degenerative process in the brain.
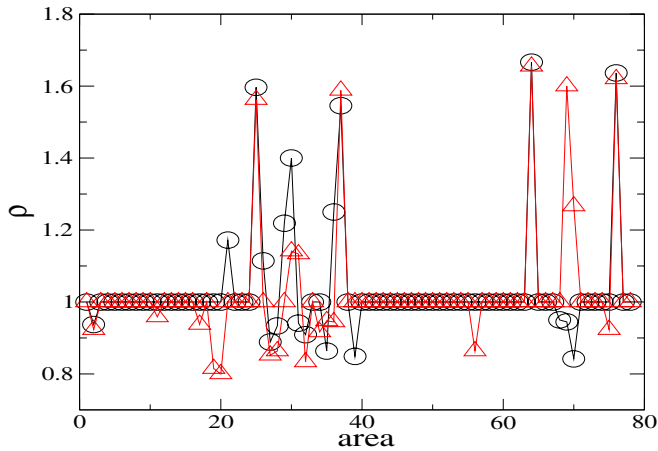
Fig. 4. Local rich club for the areas in the HD (black circles) and DM (red triangles).

3 Phase synchronisation

Neuronal groups can generate oscillatory activity, as well as they can exhibit synchronised activity [39]. In this work, as a diagnostic tool we use the order parameter to identify synchronous behaviours. The order parameter was introduced by Kuramoto [40]

$$z_n = R_n \exp(\mathrm{i}\Psi_n) \equiv \frac{1}{N_{\mathrm{neur}}} \sum_{j \in a} \exp(\mathrm{i}\psi_n^{(j, I_{\mathrm{neur}})}), \tag{8}$$

where R_n and Ψ_n are the amplitude and angle for a centroid phase vector, respectively. $\psi_n^{(j, I_{\mathrm{neur}})}$ corresponds to the phase of the neuron j belonging to the set I_{neur} with an amount of neurons N_{neur} which are considered to compute R_n. The phase is given by

$$\psi_n = 2\pi k + 2\pi \frac{n - n_k}{n_{k+1} - n_k}, \tag{9}$$

where n_k denotes when the burst starts (Fig. 1a). We calculate the average order $\overline{R}$ parameter between the areas (a, a') in the time interval T,

$$\overline{R} = \frac{1}{T} \sum_{n=1}^{T} R_n^{(a, a')}. \tag{10}$$

For identical neurons, $\overline{R} = 1$ when they are completely synchronised and $\overline{R} \ll 1$ for desynchronous behaviour. In our neuronal network, we consider that the neurons are synchronised if $\overline{R} > 0.9$, due to the fact that the neurons are not identical.

Figure 5 shows the $\overline{R}$ values between the cortical areas in the HM and DM. For $g_e = 0.02$ and $g_c = 0.002$ both HM (Fig. 5a) and DM (Fig. 5b) exhibit $\overline{R}$ values less than 0.9 as a result of the asynchronous behaviour. Increasing g_c we verify the emergence of a large region of synchronicity in the network. Figures 5c and 5d display the areas where the neurons are synchronised. We verify different synchronised areas in the HM and DM, as well as 35% and 45% of $\overline{R}$ values greater than 0.9, respectively.
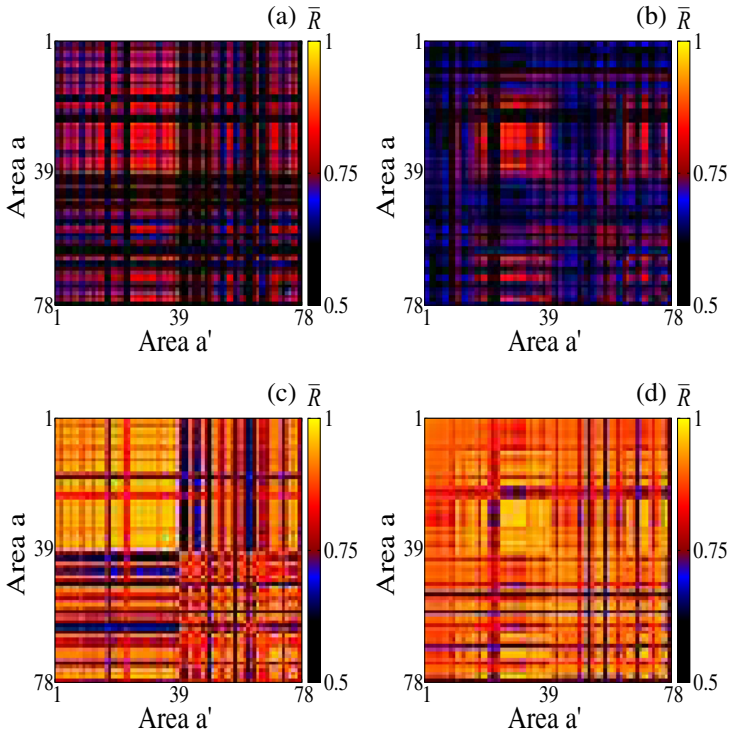
Fig. 5. Average order parameter (colour bar) for $g_c = 0.002$ in panels (a) HM and (b) DM, and $g_c = 0.004$ in panels (c) HM and (d) DM.

The occipital ($26 \leq a \leq 32$) region exhibits not only phase synchronisation in both matrices of the corticocortical connectivity, but also large values of MI. The different synchronous patterns between the matrices can be associated with the change of the rich-club organisation due to the degenerative process in the brain.

4 Delayed feedback control

The delayed feedback control was proposed by Pyragas [17]. In this control method a delayed signal from the system is used as external perturbation to change the system's dynamical behaviour. The analytical knowledge of the system is not required in feedback scheme. It was suggested for suppression of synchrony in neuronal networks [21].

In this work, we consider a delayed feedback control to suppress synchronous behaviour in both HM and DM. The delayed feedback can be introduced modifying the external perturbation in equation (3) as

$$\Lambda_n = \frac{1}{N_p} \sum_{(i,a) \in I_p} x_{n-\tau}^{(i,a)}, \tag{11}$$

where N_p is the number of neurons belonging to a set I_p of perturbed neurons, and τ is the time delay.
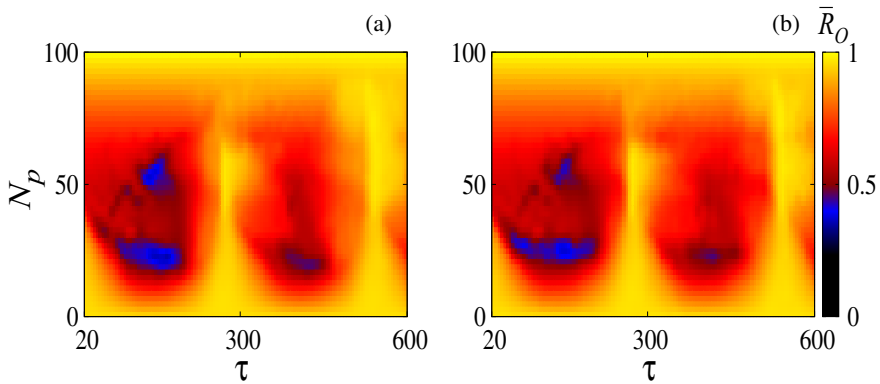
Fig. 6. $\overline{R}_O$ (colour bar) as a function of N_p and τ for $g_c = 0.004$ in panels (a) HM and (b) DM. The delayed feedback control is applied in the region $26 \leq a \leq 32$.
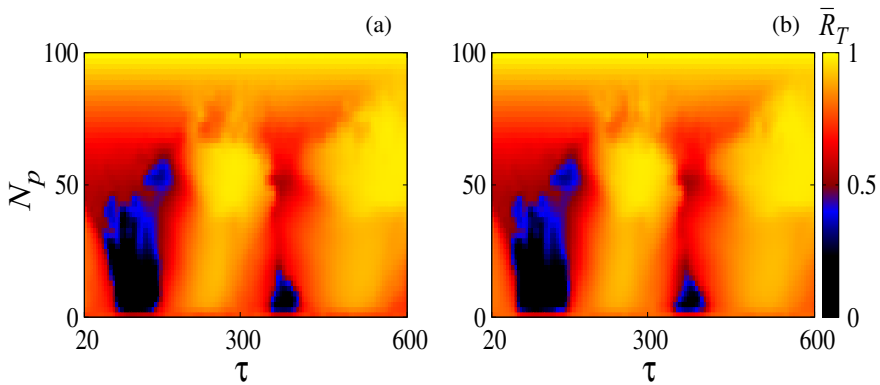

Fig. 7. $\overline{R}_T$ (colour bar) as a function of N_p and τ for $g_c = 0.004$ in panels (a) HM and (b) DM. The delayed feedback control is applied in a percentage N_p of neurons that are randomly chosen in the network of networks.

Firstly, the delayed feedback control is applied only in the occipital region. This region ($26 \leq a \leq 32$) has large MI and synchronised areas in both HM and DM. We calculate the average order parameter for the occipital region $\overline{R}_O$ as a function of N_p and τ, as shown in Figure 6, where N_p is the percentage of neurons in the occipital region. We verify the existence of domains of suppression, that are found around $N_p \approx 25$ and $N_p \approx 50$. The domains also depend on the τ values. For $\tau \approx 280$, the average time between two bursts, the feedback does not suppress the neuronal synchronisation. Whereas for $\tau \approx 140$, half of the average time between two bursts, the synchronisation is successfully suppressed.

Secondly, we apply the delayed feedback in a percentage N_p of neurons randomly chosen in all network of networks. Figure 7 displays the total average order parameter R_T as a function of N_p and τ. R_T is calculated considering all neurons in the neuronal network. We see in both HM and DM that there is one large domain of synchronisation suppression for $4 < N_p < 50$ and τ from 80 to 160.

5 Conclusion

Neuronal synchronisation plays an important role in various tasks, as well as it has been related to pathological brain rhythms. With this in mind, we build a network of networks composed by Rulkov neurons to study suppression of neuronal phase synchronisation. We consider structural connection matrices according to a healthy and degenerative brain.

Both networks exhibit synchronous behaviour among different areas when the coupling strength is increased. We observe different synchronous patterns between the matrices that are related to the change of the rich-club organisation due to the degenerative process in the brain. In addition, the occipital region has large values of MI, as well as it shows phase synchronisation in both HM and DM.

With the objective of suppressing synchronous behaviour, we apply the delayed feedback control. We find suppression domains by varying the percentage of perturbed neurons and the time delay. We verify that it is possible to suppress the synchronisation in the occipital region applying the feedback in 25% of the neurons with a τ value around 140, that is the half of average time between two bursts. Moreover, with 5% of neurons randomly chosen in the network and τ from 80 to 160 the synchronisation can be suppressed in all neuronal network. Therefore, we show that delayed feedback control can be used to suppress synchronous behaviours not only in the healthy brain, but also in the degenerative brain.

Author contribution statement

All authors contributed extensively to the work presented in this paper.

References

1. S. Grossber, Neural Netw. **1**, 17 (1988)
2. P. Dayan, L.F. Abbott, *Theoretical neuroscience: computational and mathematical modeling of neural systems* (MIT Press, Cambridge, 1999)
3. B.W. Connors, M.A. Long, Annu. Rev. Neurosci. **27**, 393 (2004)
4. S.-C. Lee, S.J. Cruikshank, B.W. Connors, J. Physiol. **588**, 2403 (2010)
5. G. Buzsáki, A. Draguhn, Science **304**, 1926 (2004)
6. R. Willemet, Brain Sci. **2**, 203 (2012)
7. P. Hangmann, L. Cammoun, X. Gigandet, R. Meuli, C.J. Honey, V.J. Wedeen, O. Sporns, PLoS Biol. **6**, e159 (2008)
8. B.T. Thomas Yeo, F.M. Krienen, J. Sepulcre, M.R. Sabuncu, D. Lashkari, M. Hollinshead, J.L. Roffman, J.W. Smoller, L. Zöllei, J.R. Polimeni, B. Fischl, H. Liu, R.L. Buckner, J. Neurophysiol. **106**, 1125 (2011)
9. M.F. Glasser, T.S. Coalson, E.C. Robinson, C.D. Hacker, J. Harwell, E. Yacoub, K. Ugurbil, J. Andersson, C.F. Beckmann, M. Jenkinson, S.M. Smith, D.C. Van Essen, Nature **536**, 171 (2016)

10. J. Fell, N. Axmacher, Nat. Rev. Neurosci. **12**, 105 (2011)
11. P.J. Uhlhaas, W. Singer, Neuron **52**, 155 (2006)
12. K. Lehnertz, J. Biol. Phys. **34**, 253 (2008)
13. R. Levy, W.D. Hutchison, A.M. Lozano, J.O. Dostrovsky, J. Neurosci. **22**, 2855 (2002)
14. C. Hammond, H. Bergman, P. Brown, Trends Neurosci. **30** 357 (2007)
15. E.L. Lameu, C.A.S. Batista, A.M. Batista, K. Iarosz, R.L. Viana, S.R. Lopes, J. Kurths. Chaos **22**, 043149 (2012)
16. E.L. Lameu, F.S. Borges, R.R. Borges, K.C. Iarosz, I.L. Caldas, A.M. Batista, R.L. Viana, J. Kurths, Chaos **26**, 043107 (2016)
17. K. Pyragas, Phys. Lett. A **170**, 421 (1992)
18. X. Li, J. C. Ji, C.H. Hansen, C. Tan, J. Sound Vib. **291**, 644 (2006)
19. Z.H. Liu, W.Q. Zhu, J. Sound Vib. **299**, 178 (2007)
20. J.A. Holyst, K. Urbanowicz, Physica A **287**, 587 (2000)
21. M. Rosenblum, A. Pikovsky, Phys. Rev. E **70**, 041904 (2004)
22. C.A.S. Batista, S.R. Lopes, R.L. Viana, A.M. Batista, Neural Netw. **23**, 114 (2010)
23. F.A.S. Ferrari, R.L. Viana, A.S. Reis, K.C. Iarosz, I.L. Caldas, A. M. Batista, Physica A **496**, 162 (2018)
24. C. Hauptmann, J.-C. Roulet, J.J. Niederhauser, W. Döll, M.E. Kirlangic, B. Lysyansky, V. Krachkovskyi, M.A. Bhatti, U.B. Barnikol, L. Sasse, C.P. Bührle, E.-J. Speckmann, M. Götz, V. Sturm, H.-J. Freund, U. Schnell, P.A. Tass, J. Neural Eng. **6**, 066003 (2009)
25. O.V. Popovych, P.A. Tass, Front. Physiol. **9**, 1 (2018)
26. O.V. Popovych, B. Lysyansky, M. Rosenblum, A. Pikovsky, P.A. Tass, PLoS One **12**, e0173363 (2017)
27. A. Berényi, M. Belluscio, D. Mao, G. Buzsáki, Science **337**, 735 (2012)
28. G. van Luijtelaar, A. Lüttjohann, V.V. Makarov, V.A. Maksimenko, A.A. Koronovskii, A.E. Hramov, J. Neurosci. Methods **260**, 144 (2016)
29. V.A. Maksimenko, S. van Heukelum, V.V. Makarov, J. Kelderhuis, A. Lüttjohann, A.A. Koronovskii, A.E. Hramov, G. van Luijtelaar, Sci. Rep. **7**, 2487 (2017)
30. C.-Y. Lo, P.-N. Wang, K.-H. Chou, J. Wang, Y. He, C.-P. Lin, J. Neurosci. **30**, 16876 (2010)
31. D.J. Watts, S.H. Strogatz, Nature **393**, 440 (1998)
32. Y. He, Z.J. Chen, A.C. Evans, Cereb. Cortex **17**, 2407 (2007)
33. N.F. Rulkov, Phys. Rev. Lett. **86**, 183 (2001)
34. C.A.S. Batista, E.L. Lameu, A.M. Batista, S.R. Lopes, T. Pereira, G. Zamora-López, J. Kurths, R.L. Viana, Phys. Rev. E **86**, 016211 (2012)
35. E.L. Lameu, F.S. Borges, R.R. Borges, A.M. Batista, M.S. Baptista, R.L. Viana, Commun. Nonlinear Sci. Numer. Simul. **34**, 45 (2016)
36. M.E.J. Newman, D.J. Watts, Phys. Rev. E **60**, 7332 (1999)
37. C.C. Hilgetag, R. Kötter, K.E. Stephan, O. Sporns, *Computational neuroanatomy* (Humana Press, Totowa, 2002)
38. T. Opsahl, V. Colizza, P. Panzarasa, J.J. Ramasco, Phys. Rev. Lett. **101**, 168702 (2008)
39. E. Lowet, M.J. Roberts, P. Bonizzi, J. Karel, P.D. Weerd, PLoS One **11**, e0146443 (2016)
40. Y. Kuramoto, *Chemical oscillations, waves, and turbulence* (Springer, Berlin, 1984)